

Polarization-sensitive absorption of THz radiation by interacting electrons in chirally stacked multilayer graphene

Maxim Trushin and John Schliemann

Institute for Theoretical Physics, University of Regensburg, D-93040 Regensburg, Germany

We show that opacity of a clean multilayer graphene flake depends on the helicity of the circular polarized electromagnetic radiation. The effect can be understood in terms of the pseudospin selection rules for the interband optical transitions in the presence of exchange electron-electron interactions which alter the pseudospin texture in momentum space. The interactions described within a semi-analytical Hartree-Fock approach lead to the formation of the topologically different broken-symmetry states characterized by Chern numbers and zero-field anomalous Hall conductivities.

I. INTRODUCTION

Multilayer graphene is a link between one atom thick carbon layers¹ with the peculiar Dirac-like effective Hamiltonian for carriers² and graphite³ which can be seen as millions of graphene layers stacked together. Graphene layers placed together do not lie exactly one on top of each other but are shifted in such a way that only half of the carbon atoms have a neighbor in another layer and the other half are projected right into the middle of the graphene's "honeycomb cell". If the third layer aligns with the first (and the $n+2$ layer with the n -th) then we arrive at the more stable arrangement of graphene layers known as Bernal (or AB) stacking, see Fig. 1a. However, this is not the only possible configuration. One can imagine an alternative stacking when the third layer aligns neither the first nor the second but shifted with respect to both, see Fig. 1b. This arrangement is known as rhombohedral (or ABC) stacking and represents the main topic of this work.

The very first studies of Bernal and rhombohedral graphites³⁻⁷ relying on the tight binding model have demonstrated the strong dependence of the band structure on the stacking order. Later on the progress in numerical methods made it possible to refine the tight binding model outcomes using *ab initio* calculations⁸⁻¹⁰. The seminal transport measurements on graphene¹¹ have inspired recent investigations¹²⁻¹⁴ of the band structure in a few layer graphene having different stacking patterns. The band structure demonstrates a large variety of behavior including a gapless spectrum, direct and indirect band gaps, and energetic overlap of the conduction and valence bands even though the number of layers has been limited by four.¹² In addition, the Landau levels and electric field induced gap in a few layer graphene have been studied in Refs.¹³ and¹⁴ respectively. A very interesting effect of Landau-level crossing has been found very recently in trilayer graphene.¹⁵ It has also been shown that electron-electron interaction effects play an important role in a few layer graphene where charge carriers may exhibit a variety of broken symmetry states.¹⁶

The brief literature overview given above illustrates how rich the band structure of multilayer graphene (and the effects associated with) can be. Note, how-

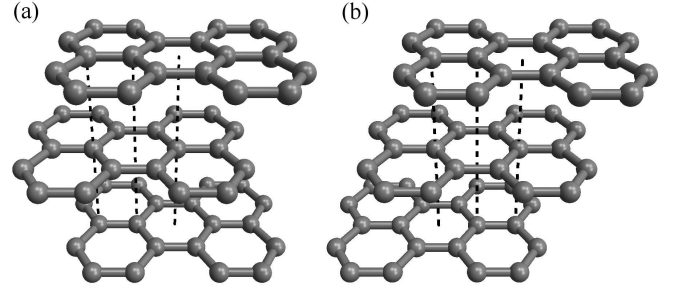


FIG. 1: (a) Bernal graphite represents graphene layers placed together in ...-AB-AB-AB-... stacking when the two layers shifted with respect to each other by 0.142 nm alternate in bulk. (b) Rhombohedral graphite requires three non-equivalent graphene layers when the two layers are shifted with respect to the first one by 0.142 nm and 0.284 nm alternating in ...-ABC-ABC-ABC-... sequence. Dashed lines are shown for an eye guide.

ever, that among all stacking possibilities, only the pure ABC arrangement maintains the sublattice pseudospin chirality.¹⁷ In the simplest case of negligible interlayer asymmetries and trigonal warp the simplified two-band ABC graphene model leads to the following Hamiltonian close to the neutrality point¹⁷

$$H_0^\nu = \frac{(\hbar v_0)^N}{(-\gamma_1)^{N-1}} \begin{pmatrix} 0 & (\nu k_x - i k_y)^N \\ (\nu k_x + i k_y)^N & 0 \end{pmatrix}, \quad (1)$$

where $v_0 \approx 10^6 \text{ ms}^{-1}$ is the group velocity for carriers in single layer graphene, γ_1 is the hopping parameter, $\nu = \pm$ is the valley index, and N is the number of layers. As one can see from Eq. (1), the N -layer and $(N+1)$ -layer graphene stacks differ, apart from the density of states, by only the winding number associated with the pseudospin orientation. The pseudospin texture in the momentum space associated with Hamiltonian (1) and shown in Fig. 2 is the main topic of this work. In what follows we focus on the influence of electron-electron exchange interactions on the pseudospin texture and its detection by optical means.

Note that the pseudospin lies in the xy -plane as long as its carrier remains in an eigenstate of H_0^ν . The exchange

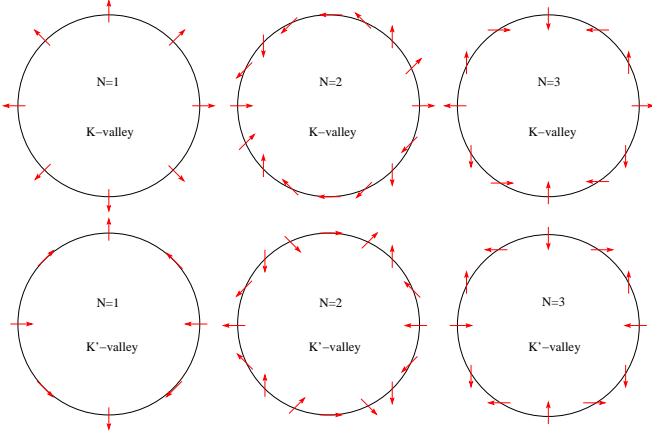


FIG. 2: Top view on the pseudospin texture for the conduction band in chirally stacked multilayer graphene calculated from the non-interacting Hamiltonian (1). The pseudospin orientations in conduction and valence bands for a given momentum are antiparallel.

interactions can turn the pseudospin texture to the out-of-plane phase with the out-of-plane angle depending on the absolute value of the particle momentum^{16,18–20}. This is due to the huge negative contribution to the Hartree–Fock ground state energy from the valence band (i. e. “antiparticle” states) which cannot be neglected in graphene because of the zero gap and conduction-valence band coupling via pseudospin. The broken symmetry states in multilayer graphene with chiral stacking have been recently studied by Zhang *et al*¹⁶ using quite general arguments. Spontaneous symmetry breaking can occur in presence of exchange electron-electron interactions²⁰. Here, we utilize a simplified model which includes exchange electron-electron interactions but, at the same time, allows transparent half-analytical solution. Having this solution at hand we focus on the manifestation of such broken symmetry states in optical absorption measurements.

Optical absorption via the direct interband optical transitions in monolayer graphene has been investigated in²¹ and shown to be equal to the universal value $\pi e^2/\hbar c$. In the presence of the electron-electron interactions the interband absorption can be substantially reduced or enhanced as compared to its universal value $\pi e^2/\hbar c$ just by switching the helicity of the circularly polarized light¹⁸. This effect is due to the peculiar pseudospin texture arising from the interplay between pseudospin-momentum coupling and exchange interactions. To observe the pseudospin texture in chirally stacked multilayer graphene by optical means the photon energy must be much smaller than the bottom of the lowest split-off bands $\gamma_1 = 0.4$ eV. To give an example, a CH₃OH 20 mW laser²² with wavelength $118 \mu\text{m}$ (i.e. with the photon energy 10.5 meV) safely satisfies this condition.

II. MODEL

We start from the Coulomb exchange Hamiltonian for chiral carriers which is given by

$$H_{\text{exch}}^\nu(\mathbf{k}) = - \sum_{\kappa'} \int \frac{d^2 k'}{4\pi^2} U_{|\mathbf{k}-\mathbf{k}'|} |\chi_{\kappa'\kappa'}^\nu\rangle \langle \chi_{\kappa'\kappa'}^\nu| \quad (2)$$

with $U_{|\mathbf{k}-\mathbf{k}'|} = 2\pi e^2/\varepsilon|\mathbf{k}-\mathbf{k}'|$ and $\kappa' = \pm$ being the band index with $\kappa = +$ for the conduction band. In order to consider the exchange Hamiltonian for any N on the equal footing we assume strictly two-dimensional Fourier transform for Coulomb potential. This is in contrast to²⁰ where the interlayer distance d has been included in the screening multiplier. The intervalley overlap is assumed to be negligible, and the eigenstates of $H^\nu = H_0^\nu + H_{\text{exch}}^\nu$ can be formulated as $\Psi_{\mathbf{k}\kappa}^\nu(\mathbf{r}) = e^{i\mathbf{k}\mathbf{r}} |\chi_{\kappa\kappa}^\nu\rangle$ with spinors $|\chi_{\kappa+}^\nu\rangle = (\cos \frac{\vartheta_k}{2}, \nu \sin \frac{\vartheta_k}{2} e^{i\nu N\varphi})^T$, $|\chi_{\kappa-}^\nu\rangle = (\sin \frac{\vartheta_k}{2}, -\nu \cos \frac{\vartheta_k}{2} e^{i\nu N\varphi})^T$, and $\tan \varphi = k_y/k_x$, where a non-zero out-of-plane pseudospin component corresponds to $\vartheta_k \neq \pi/2$. To diagonalize H^ν the following ν -independent equation for ϑ_k must be satisfied^{18,23}

$$\frac{(\hbar v_0 k)^N}{(-\gamma_1)^{N-1}} \cos \vartheta_k + \sum_{\kappa'} \int \frac{d^2 k'}{8\pi^2} \kappa' U_{|\mathbf{k}-\mathbf{k}'|} [\cos \vartheta_{k'} \sin \vartheta_k - \sin \vartheta_{k'} \cos \vartheta_k \cos(N\varphi' - N\varphi)] = 0. \quad (3)$$

Here the integration goes over the occupied states. Note that the conduction and valence states are entangled, and the latter cannot be disregarded even at positive Fermi energies assumed below. Thus, in order to evaluate the integrals in Eq. (3) a momentum cut-off Λ is necessary. Most natural choice $\Lambda = \gamma_1/\hbar v_0$ corresponds to the energy scale γ_1 at which the split-off bands of bilayer graphene become relevant and our two-band model no longer applies. Substituting $x = k/\Lambda$ we arrive at

$$\frac{4\pi}{\alpha^*} x^N \cos \vartheta_k = \int_0^{2\pi} d\varphi' \int_{k_F/\Lambda}^1 dx' x' \frac{\cos \vartheta_{k'} \sin \vartheta_k - \sin \vartheta_{k'} \cos \vartheta_k \cos N\varphi'}{\sqrt{x^2 + x'^2 - 2xx' \cos \varphi'}}, \quad (4)$$

where $\alpha^* = e^2/(\varepsilon \hbar v_0)$. The momentum cut-off is assumed to be much larger than the Fermi momentum k_F , and, therefore, we can set the lower integral limit to zero. In this case our outcomes do not depend on the value of Λ .

Besides a trivial solution with $\vartheta_0 = \pi/2$ independent of k , there are non-trivial ones $\vartheta_1 = \vartheta(k)$ and $\vartheta_2 = \pi - \vartheta(k)$ with $\vartheta(k)$ shown in Figs. 3a and 4a for different N and α^* . The solutions ϑ_0 and $\vartheta_{1,2}$ represent to two phases with different total ground state energies $E_{\text{tot}}^{\text{in}}$ ($E_{\text{tot}}^{\text{out}}$) for the in-plane (out-of-plane) pseudospin phase. The difference

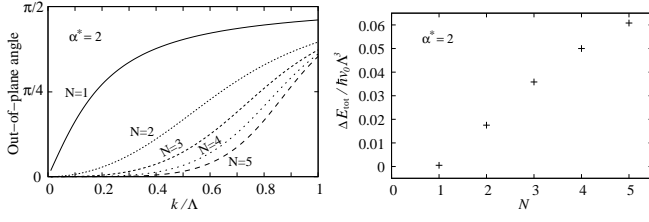


FIG. 3: Left panel: The pseudospin out-of-plane angle $\vartheta(k)$ for substrate-free chirally stacked N -layer graphene numerically calculated from Eq. (4). Right panel: The total ground state energy difference (5) between the in-plane and out-of-plane phases for different N . Increasing N makes the out-of-plane phase more preferable. The $\vartheta(k)$ curve for $N = 1$ differs from the one given in¹⁸ since we have improved the precision of our calculations here. Note, that the Coulomb interactions are completely unscreened here. The screening is taken into account in Fig. 4 by introducing the effective dielectric constant ϵ which relates to α^* as $\alpha^* = e^2/(\epsilon \hbar v_0)$.

$\Delta E_{\text{tot}} = E_{\text{tot}}^{\text{in}} - E_{\text{tot}}^{\text{out}}$ per volume is given by

$$\begin{aligned} \frac{\Delta E_{\text{tot}}}{\hbar v_0 \Lambda^3} = & -\frac{g_s g_v}{2\pi} \int_0^1 dx' x'^{N+1} (1 - \sin \vartheta_{k'}) \\ & - \alpha^* \frac{g_s g_v}{32\pi^3} \int_0^{2\pi} d\varphi \int_0^{2\pi} d\varphi' \int_0^1 dx \int_0^1 dx' \\ & \frac{xx' (1 - \sin \vartheta_{k'} \sin \vartheta_k) \cos(N\varphi' - N\varphi) - \cos \vartheta_{k'} \cos \vartheta_k}{\sqrt{x^2 + x'^2 - 2xx' \cos(\varphi - \varphi')}}. \end{aligned} \quad (5)$$

The ground state energy is the same for *both* valleys and spins, and, therefore, Eq. (5) contain $g_s = 2$ and $g_v = 2$ for spin and valley degeneracy respectively. ΔE_{tot} has been evaluated numerically and the resulting ΔE_{tot} vs. N dependency is shown in Figs. 3b and 4b for suspended and SiO₂-placed graphene respectively. One can see that strong electron-electron interactions with $\alpha^* = 2$ definitely make the out-of-plane phase energetically preferable for $N > 1$. For graphene placed on SiO₂ substrate the pseudospin out-of-plane phase is energetically preferable only for $N \geq 3$. Note that the estimates of α^* for clean monoatomic graphene flake vary from 2 (Ref.²⁴) to 2.8 (Ref.²⁵) and, therefore, even monolayer graphene may get to the pseudospin out-of-plane phase.

Note that it is possible to choose either the same or opposite solutions for two valleys. The former choice breaks the parity invariance whereas the latter one does so with the time reversal symmetry.¹⁸ In what follows we consider possible manifestations of these solutions in the optical absorption measurements on multilayer graphene.

III. OPTICAL ABSORPTION

We assume that an electromagnetic wave is propagating along z axis perpendicular to graphene plane. It can

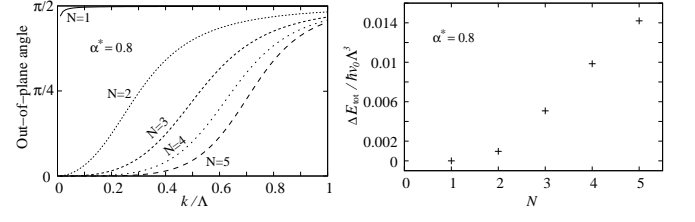


FIG. 4: Left panel: The pseudospin out-of-plane angle $\vartheta(k)$ for chirally stacked N -layer graphene on SiO₂ numerically calculated from Eq. (4). Right panel: The total ground state energy difference (5) between the in-plane and out-of-plane phases for different N . The difference is much larger in the case of substrate-free graphene, see Fig. 3.

be described by the electric field $\mathbf{E} = \mathbf{E}_0 \exp(ik_z z - i\omega t)$, where k_z is the wave vector, and ω is the radiation frequency. For our purpose it is more convenient to characterize the electromagnetic wave by its vector potential $\mathbf{A} = \mathbf{A}_0 \exp(ik_z z - i\omega t)$, where $\mathbf{A}_0 = i\epsilon \mathbf{E}/\omega$. The relation between \mathbf{E} and \mathbf{A} is unambiguous since \mathbf{A} is always in xy plane resulting in a gauge with $\text{div} \mathbf{A} = 0$. The interaction Hamiltonian can be then written in the lowest order in \mathbf{A} as

$$\begin{aligned} H_{\text{int}}^\nu = & \frac{(\nu \hbar v_0 k)^N}{k(-\gamma_1)^{N-1}} \frac{eN}{\hbar c} \\ & \times \begin{pmatrix} 0 & e^{-\nu i\varphi(N-1)}(A_x - i\nu A_y) \\ e^{\nu i\varphi(N-1)}(A_x + i\nu A_y) & 0 \end{pmatrix}. \end{aligned} \quad (6)$$

The total absorption P can be calculated as a ratio between the total electromagnetic power absorbed by graphene per unit square $W_a = \hbar \omega \sum_\nu \int \frac{d^2 k}{4\pi^2} w(\mathbf{k}+, \mathbf{k}-)$ and the incident energy flux $W_i = \omega^2 A^2 / 4\pi c$. The probability to excite an electron from the valence band to an unoccupied state in the conduction band $w(\mathbf{k}+, \mathbf{k}-)$ can be calculated using Fermi's golden-rule

$$w(\mathbf{k}+, \mathbf{k}-) = \frac{2\pi}{\hbar} |\langle \mathbf{k}+ | H_{\text{int}}^\nu | \mathbf{k}- \rangle|^2 \delta(E_{k+} - E_{k-} - \hbar \omega).$$

Because of normal incidence there is zero momentum transfer from photons to electrons. What is important is that the inter-band transition matrix elements of H_{int}^ν turn out to be sensitive to the light polarization and pseudospin orientations in the initial and final states. In particular, for linear polarization with $A_x = A \cos \varphi_{\text{pol}}$ and $A_y = A \sin \varphi_{\text{pol}}$ the probability to excite an electron with a given momentum reads

$$\begin{aligned} w(\mathbf{k}+, \mathbf{k}-)_{|\nu=+} = & \frac{\pi}{\hbar} \left(\frac{eN}{\hbar c} A \right)^2 \frac{(\hbar v_0)^{2N} k^{2N-2}}{(-\gamma_1)^{2N-2}} \\ & \times \delta(E_{k+} - E_{k-} - \hbar \omega) \\ & \times [1 + \cos^2 \vartheta_k - \sin^2 \vartheta_k \cos(2N\varphi - 2N\varphi_{\text{pol}})]. \end{aligned} \quad (7)$$

Note that $w(\mathbf{k}+, \mathbf{k}-)$ does not depend on the valley index ν . The total optical absorption P is not sensitive to

the particular orientation of the polarization plane since the φ_{pol} -dependent term is integrated out in this case. In contrast, if we assume a circular polarization fulfilling $A_x = \pm iA/\sqrt{2}$, $A_y = A/\sqrt{2}$ then the interband transition probability for K-valley can be written as

$$w(\mathbf{k}+, \mathbf{k}-)|_{\nu=+} = \frac{4\pi}{\hbar} \left(\frac{eN}{\hbar c} A \right)^2 \frac{(\hbar v_0)^{2N} k^{2N-2}}{(-\gamma_1)^{2N-2}} \times \left\{ \frac{\sin^4 \frac{\vartheta_k}{2}}{\cos^4 \frac{\vartheta_k}{2}} \right\} \delta(E_{k+} - E_{k-} - \hbar\omega). \quad (8)$$

Here, the multipliers $\sin^4(\vartheta_k/2)$ and $\cos^4(\vartheta_k/2)$ are for two opposite helicities of light, and for K'-valley they are interchanged. If the out-of-plane pseudospin polarization is chosen to be opposite in two valleys then this helicity dependence survives the integration over momentum and summation over valley index resulting in the helicity-sensitive total absorption which reads

$$P = \frac{16N^2}{\hbar\omega} \frac{\pi e^2}{\hbar c} \frac{(\hbar v_0)^{2N}}{(-\gamma_1)^{2N-2}} \times \int_0^\Lambda dk k^{2N-1} \left\{ \frac{\sin^4 \frac{\vartheta_k}{2}}{\cos^4 \frac{\vartheta_k}{2}} \right\} \delta(E_{k+} - E_{k-} - \hbar\omega). \quad (9)$$

The absorption strongly depends on helicity as long as the radiation frequency is much smaller than the band split-off energy. This regime corresponds to the excitation of electrons with comparatively small momenta, where the angle ϑ_k is close to zero, see Fig. 3b and Fig. 4b.

The experiment proposed here is similar to the one discussed recently in Ref.²⁶ suggesting to detect broken symmetry states in graphene placed on substrate by polar Kerr rotation measurements, i.e. by analyzing the elliptical polarization of reflected radiation. In the present paper, however, we propose to reach the same goal by comparing the opacity for two orthogonal light polarizations, which appears to be the simpler strategy.

Alternatively, one can characterize broken-symmetry states in terms of the topological Chern numbers²⁷ given by

$$n_\pm^\nu = \frac{1}{2\pi} \int d^2k \nabla_k \times \mathbf{A}_\pm^\nu \quad (10)$$

with $\mathbf{A}_\pm^\nu = i\langle \chi_{k\pm}^\nu | \nabla_k | \chi_{k\pm}^\nu \rangle$. This approach is routinely used in the theory of topological insulators²⁸ and originated from the description of quantized Hall conductances.

A non-trivial band topology has also been found in graphene^{29,30} where the band gap was opened via spin-orbit coupling characterized just by a constant (i.e. wave vector independent) mass term rather than by exchange interactions described by a more complicated Hamiltonian (2).

Note, that in our case here $\nabla_k \times \mathbf{A}_\pm^\nu$ contains a term proportional to $\delta(\mathbf{k})$ which occurs due to the singularity

in $\mathbf{A}_\pm^\nu \propto k^{-1}$ but does not contribute to n_\pm^ν as long as $\vartheta_k = 0$ at $k \rightarrow 0$. Thus, for the conduction band electrons we have

$$n_+^\nu = -\frac{\nu N}{2} \int_{\vartheta(0)}^{\vartheta(\Lambda)} d\vartheta_k \sin \vartheta_k. \quad (11)$$

Assuming the out-of-plane pseudospin polarization to be opposite in two valleys it follows that the total Chern number for conduction electrons just equals N . On the other hand, the total Chern number is zero as long as the out-of-plane pseudospin pseudospin component is same in both valleys. Thus, the two out-of-plane solutions are *topologically* different even though they correspond to the band gap of the same size. The topologically non-trivial case with $n \neq 0$ corresponds to broken time reversal symmetry leading to the existence of a zero-field Hall current¹⁸.

The only question is whether the time reversal broken states really occur in clean graphene samples. More in depth analysis performed by Nandkishore and Levitov^{26,31} suggests that this is the case at least for bilayer graphene. On the other hand Jung *et al.*¹⁹ demonstrate that the intervalley exchange coupling favors parallel pseudospin polarization in opposite valleys breaking the parity invariance. In this case the total absorption does not depend on the radiation helicity but the two valleys are occupied differently by the photoexcited carriers which might be useful effect for *valleytronics*³².

In the in-plane phase with $\vartheta = \pi/2$ the total absorption does not depend on light polarization, and in the non-interacting limit it equals to

$$P = N \frac{\pi e^2}{\hbar c} \quad (12)$$

At $N = 1$ it acquires the universal value $\frac{\pi e^2}{\hbar c}$, as expected²¹.

IV. CONCLUSION

We have demonstrated that the polarization-sensitive optical absorption predicted in¹⁸ for single layer graphene can be found in chirally stacked carbon multilayers within a broader range of parameters. This is due to the enhancement of the interaction effects in multilayer graphene with larger number of layers. The conditions necessary for the observation of the polarization-dependent optical absorption can be summarized as follows. (i) Graphene samples must be prepared as cleaner as possible. It would be better to utilize suspended samples in order to isolate the interacting electrons from the environment with large relative permittivity. (ii) The exchange interactions must break the time reversal invariance rather than the parity. This situation corresponds to the topologically non-trivial state with the Chern number equal to N . (iii) Finally, the low frequency radiation

is necessary to excite the electrons with smaller momenta having larger out-of-plane pseudospin components and to preclude the influence of split-off bands.

In addition, we would like to mention the possible existence of a zero-field Hall current in the slightly doped graphene samples where the time reversal invariance is broken as described above.

Acknowledgements

We would like to thank Tobias Stauber, Jeil Jung, and Fan Zhang for stimulating discussions. This work was supported by DFG via GRK 1570.

-
- ¹ K. S. Novoselov, A. K. Geim, S. V. Morozov, D. Jiang, M. I. Katsnelson, I. V. Grigorieva, S. V. Dubonos, and A. A. Firsov, *Nature* **438**, 197 (2005).
 - ² A. H. Castro Neto, F. Guinea, N. M. R. Peres, K. S. Novoselov, and A. K. Geim, *Rev. Mod. Phys.* **81**, 109 (2009).
 - ³ P. R. Wallace, *Phys. Rev.* **71**, 622 (1947).
 - ⁴ J. W. McClure, *Phys. Rev.* **108**, 612 (1957).
 - ⁵ J. C. Slonczewski and P. R. Weiss, *Phys. Rev.* **109**, 272 (1958).
 - ⁶ R. R. Haering, *Canadian Journal of Physics* **36**, 352 (1958).
 - ⁷ J. W. McClure, *Carbon* **7**, 425 (1969).
 - ⁸ G. S. Painter and D. E. Ellis, *Phys. Rev. B* **1**, 4747 (1970).
 - ⁹ D. Tománek and S. G. Louie, *Phys. Rev. B* **37**, 8327 (1988).
 - ¹⁰ J.-C. Charlier, X. Gonze, and J.-P. Michenaud, *Phys. Rev. B* **43**, 4579 (1991).
 - ¹¹ K. S. Novoselov, A. K. Geim, S. V. Morozov, D. Jiang, Y. Zhang, S. V. Dubonos, I. V. Grigorieva, and A. A. Firsov, *Science* **306**, 666 (2004).
 - ¹² S. Latil and L. Henrard, *Phys. Rev. Lett.* **97**, 036803 (2006).
 - ¹³ F. Guinea, A. H. Castro Neto, and N. M. R. Peres, *Phys. Rev. B* **73**, 245426 (2006).
 - ¹⁴ A. A. Avetisyan, B. Partoens, and F. M. Peeters, *Phys. Rev. B* **81**, 115432 (2010).
 - ¹⁵ T. Taychatanapat, K. Watanabe, T. Taniguchi, and P. Jarillo-Herrero, *Nat. Phys.* **7**, 621 (2011).
 - ¹⁶ F. Zhang, J. Jung, G. A. Fiete, Q. Niu, and A. H. MacDonald, *Phys. Rev. Lett.* **106**, 156801 (2011).
 - ¹⁷ F. Zhang, B. Sahu, H. Min, and A. H. MacDonald, *Phys. Rev. B* **82**, 035409 (2010).
 - ¹⁸ M. Trushin and J. Schliemann, *Phys. Rev. Lett.* **107**, 156801 (2011).
 - ¹⁹ J. Jung, F. Zhang, and A. H. MacDonald, *Phys. Rev. B* **83**, 115408 (2011).
 - ²⁰ H. Min, G. Borghi, M. Polini, and A. H. MacDonald, *Phys. Rev. B* **77**, 041407 (2008).
 - ²¹ R. R. Nair, P. Blake, A. N. Grigorenko, K. S. Novoselov, T. J. Booth, T. Stauber, N. M. R. Peres, and A. K. Geim, *Science* **320**, 1308 (2008).
 - ²² J. Karch, P. Olbrich, M. Schmalzbauer, C. Brinsteiner, U. Wurstbauer, M. Glazov, S. Tarasenko, E. Ivchenko, D. Weiss, J. Eroms, et al., *Photon helicity driven electric currents in graphene*, *arxiv: 1002.1047*.
 - ²³ L. O. Juri and P. I. Tamborenea, *Phys. Rev. B* **77**, 233310 (2008).
 - ²⁴ C. Jang, S. Adam, J.-H. Chen, E. D. Williams, S. Das Sarma, and M. S. Fuhrer, *Phys. Rev. Lett.* **101**, 146805 (2008).
 - ²⁵ N. M. R. Peres, F. Guinea, and A. H. Castro Neto, *Phys. Rev. B* **72**, 174406 (2005).
 - ²⁶ R. Nandkishore and L. Levitov, *Phys. Rev. Lett.* **107**, 097402 (2011).
 - ²⁷ D. J. Thouless, M. Kohmoto, M. P. Nightingale, and M. den Nijs, *Phys. Rev. Lett.* **49**, 405 (1982).
 - ²⁸ M. Z. Hasan and C. L. Kane, *Rev. Mod. Phys.* **82**, 3045 (2010).
 - ²⁹ C. L. Kane and E. J. Mele, *Phys. Rev. Lett.* **95**, 226801 (2005).
 - ³⁰ E. Prada, P. San-Jose, L. Brey, and H. Fertig, *Solid State Communications* **151**, 1075 (2011).
 - ³¹ R. Nandkishore and L. Levitov, *Phys. Rev. B* **82**, 115124 (2010).
 - ³² D. Xiao, W. Yao, and Q. Niu, *Phys. Rev. Lett.* **99**, 236809 (2007).